International Journal of Scientific Research in Chemical Sciences **Research Paper**
Vol.6, Issue.5, pp.19-25, December (2019) **E-ISSN:** 2455-3174

Conjugation of Organic Dyes Onto pH Insensitive Silver Nanoparticles for pH Sensing

J.A. Owusu[1], K.E. Pobee-Quaynor[2*]

[1,2]Dept. of Chemical Engineering and Technology, School of Environmental and Chemical Engineering, Jiangsu University of Science and Technology, Zhenjiang, China

**Corresponding Author: kodwopobee@yahoo.com, Tel: +4915210470147*

Available online at: www.isroset.org

Received: 11/Oct/2019, Accepted: 20/Nov/2019, Online: 31/Dec/2019

Abstract **-** pH is a very important parameter in research, production and quality assessment in the fields of life sciences, pharmaceuticals and food industries. Over the years, several methods have been employed to enhance the sensing of pH. This article, however, concentrates on using fluorescence-based nanosensor detection due to its high spatial resolution, fast response, high sensitivity, simple usage and versatility to other detection schemes. Herein, a 2nm size G-AgNPs were synthesized and conjugated to a well-known pH-sensitive dye (NHS-FAM) and a pH insensitive dye (NHS-TAMRA) to produce a fluorescent pH nanoprobe sensor. After conjugating NHS-FAM to G-AgNPs, it showed an increment in fluorescent intensity over a wide range of pH values which led to an R^2 value of 0.9992. NHS-TAMRA conjugated onto the as-prepared AgNPs also showed increment in fluorescent intensity over pH values of 5-10 which resulted in linear regression (R^2) value of 0.9866.

Keywords **-** pH, Silver nanoparticles, NHS – 5(6) – carboxytetramethylrhodamine N-succinimidyl ester, 5(6) – carboxytetramethylrhodamine N-succinimidyl ester, Fluorescence, Nanoprobe.

I. INTRODUCTION

Nanotechnology is the aspect of science and engineering addressing nanomaterials that possess dimensional range between 1nm to 100th of nm [1], [2]. In the last few years, nanotechnology has been widely accepted by industrial sectors as a result of its formidable applications in the area of biotechnology, electronic storage systems [3], targeted drug delivery, magnetic separation and pre-concentration of target analytes, and medium for gene and drug delivery [4], [5].

Silver nanoparticles (AgNPs) are a class of nanomaterials that gained much interest in recent years due to its attractive physical, chemical and biological properties [6], [7]. They also possess unique physicochemical properties in terms of toxicity, electrical resistance, chemical stability, catalytic activity and surface plasmon resonance [8]. These properties have led to several applications including drug delivery, biological imaging [9], medical diagnostics and therapeutics [10], chemical and biochemical sensing [11], optical sensors, cosmetics and also in industries such as food and pharmaceutical [12]. Moreover, among several metal nanoparticles, AgNPs exhibit many advantages which include high extinction coefficients, sharper extinction bands, a higher ratio of scattering to extinction and extremely high field enhancement [13]. AgNPs are normally produced or synthesized in various forms, such as particles, rods, wires, film, and coating [14].

In pH determination in live cells, several methods have been developed, however, fluorescence spectroscopy possesses advantages due to their high spatial and temporal observation of pH changes [15], minimal invasiveness and applicability to a wide range of cells [16]. In recent years, series of fluorescence-based nanosensors have been developed for intracellular pH sensing and has since become the most widely exploited research area for pH sensing technology [17], [18], because of its high sensitivity [19], [20], tend to be operationally simple and versatility with respect to other detection schemes [21].

Herein, we present a rapid, simple and cheap method of preparing G-AgNPs by the chemical method using GSH and NaBH4 as the stabilizer and reducing agent respectively. Finally, the as-prepared G-AgNPs were tested for its reversible pH sensing properties after conjugating with a pH-sensitive dye (NHS-FAM) and a pH insensitive dye (NHS-TAMRA).

II. MATERIALS AND METHODS

AgNP SYNTHESIS

The chemical approach to G-AgNP synthesis was used. Firstly, 97ml of deionized water was measured into a three-neck bottom flask, 2ml of 100mM $AgNO_3$ was then added with constant stirring. 1ml of 200mM GSH solution was added to the three-neck bottom flask and the solution becomes cloudy. The pH of the solution was adjusted using about 60µL of 5M NaOH and after some minutes under constant stirring, 200µL of 0.5M $NaBH_4$ was then added quickly to the solution and left for 2 days under room temperature and vigorous stirring. Purification was then performed using the dialysis machine. After dialysis, the solution was freeze-dried for about 24 hours and the powder was then collected and kept for further usage.

FG-AgNP SYNTHESIS

Powdered G-AgNPs were re-dissolved in PBS (200µL, 0.05mM) and the pH was adjusted to 8. 5(6) – carboxyfluorescein N-succinimidyl ester (NHS-FAM) was dissolved in DMSO (400µL, 4.5mM) and added to the G-AgNPs in a vial slowly whiles shaking. After the reaction was complete, an aliquot of the mixture was taken into a test tube and absolute ethanol is added in the ratio of 2:1. Vigorous shaking is applied and then centrifuged for 2mins at 16000rpm. The supernatant was discarded and the precipitate was re-dissolved in PBS and the whole centrifuge procedure was repeated for about 4 times. The solution was then passed through a Sephadex LH-20 column to remove and separate the unreacted NHS-FAM from the conjugated FG-AgNPs. The first elution phase solution was then collected and centrifuged. Gel electrophoresis was then performed and pictures were taken for bright-field image and also under fluorescence.

TG-AgNP SYNTHESIS

Powdered G-AgNPs were re-dissolved in PBS (200µL, 0.05mM) and the pH was adjusted to 8. 5(6) – carboxytetramethylrhodamine N-succinimidyl ester (NHS-TAMRA) was dissolved in DMSO (80µL, 20mM) and added to the G-AgNPs in a vial slowly whiles shaking. An aliquot of the mixture was taken into a test tube and absolute ethanol is added in the ratio of 2:1 and centrifuged for 2mins at 16000rpm. The supernatant was discarded and the precipitate was re-dissolved in PBS and the whole centrifuge procedure was repeated for about 4 times. The solution was then passed through a Sephadex LH-20 column to separate the unreacted NHS-TAMRA from the conjugated TG-AgNPs. The first elution phase solution was collected, centrifuged and the precipitate re-dissolved in PBS. The resulting solution was then put into different wells of the mold and electrophoresis was performed. After that, pictures were taken for a bright-field image and also under UV light with 365nm excitation.

III. RESULTS AND DISCUSSION

The synthesis procedure of AgNPs was briefly done by the addition of GSH to freshly prepared aqueous $AgNO_3$ solution in the ratio of 1:2. This is followed by adjusting the pH to achieve a clear solution and subsequently, freshly prepared $NaBH_4$ was added to the solution. In the first step of the synthesis process, GSH, which is a water-soluble thiol reduced $AgNO_3$ partially by binding strongly and stabilizing silver ions to form a silver-thiolate complex which is a white cloudy solution [22]. Subsequent reduction of the silver – thiolate complex with freshly prepared $NaBH_4$ led to the slow formation of AgNPs. $NaBH_4$ was added to the silver – thiolate solution quickly because of its high hygroscopic nature. It was observed that after the addition of $NaBH_4$, the solution became yellow in colour and gradually transformed from yellow to amber, from amber to brown and then finally to black colour over the course of 30mins. The solution finally became orange in colour after 2 days of constant stirring which indicated the formation of G-AgNPs. The morphology of G-AgNPs was obtained using a transmission electron microscope (TEM). As shown in figure (fig.) 1, the high-resolution transmission electron microscope (HR-TEM) image indicates a uniform size distribution of G-AgNPs with an average diameter of 2.01±0.60nm.

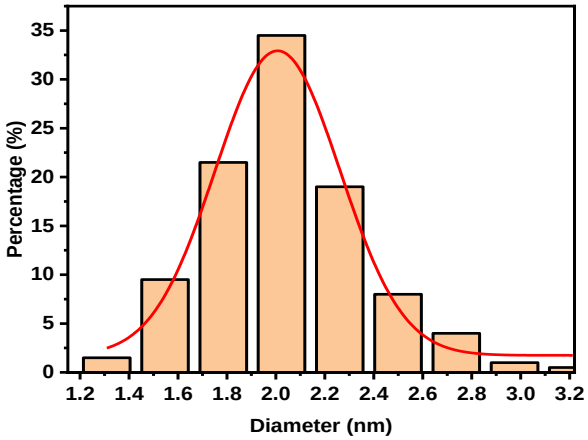

Fig. 1: HR-TEM image and size distribution of AgNP. Scale bar= 20nm

SPECTROSCOPIC ANALYSIS

After successful conjugation of NHS-FAM onto G-AgNPs, it was first confirmed using agarose gel electrophoresis. As shown in fig. 2, lane 1 represents G-AgNPs, light yellow colour in lane 2 shows FG-AgNPs and lane 3 represents the free NHS-FAM dye which is deep yellow in colour. Although all 3 lanes moved in the same direction, the G-AgNPs and FG-AgNPs moved at the same speed and at the same time from the free NHS-FAM dye. Also, comparing the bands in lane 2 and 3, it shows that the Sephadex technique successfully removed the unreacted dye. Further confirmation of conjugation was done by displaying the fluorescence image of the agarose gel under UV- light which is shown in fig. 2B. In fig. 2C, HR-TEM displayed a narrow size distribution of FG-AgNPs with an average diameter of 2.12±0.68nm which conforms with the core size of G-AgNPs (2.01±0.60nm).

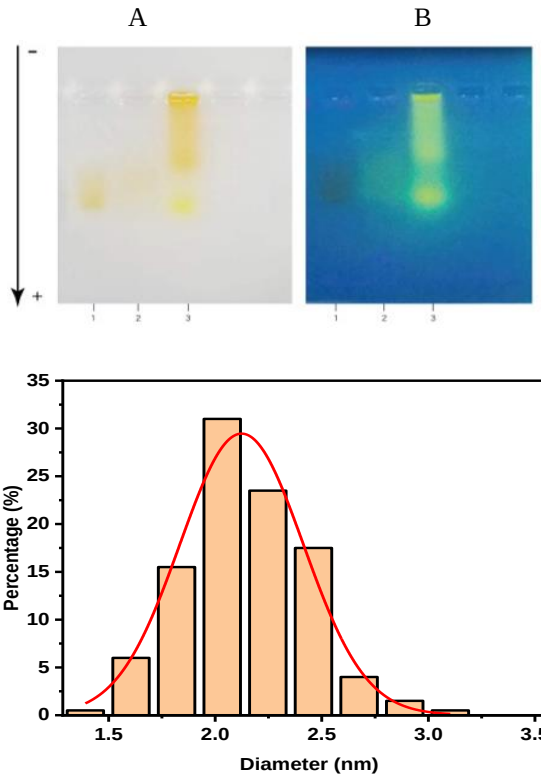

Fig. 2: Agarose gel electrophoresis of A) bright-field image B) under UV light image and C) HR-TEM image and Size distribution of FG-AgNP. Scale bar = 20nm.

Fig. 3A illustrates the absorption spectra of G-AgNP, FG-AgNP, and NHS-FAM and as shown below, NHS-FAM showed a strong absorption peak at 490nm. G-AgNPs didn't show any significant absorption hence quenching the absorption intensity of NHS-FAM when conjugated. In fig. 3B, the fluorescence spectra of NHS-FAM showed a maximum wavelength at 550nm whiles FG-AgNP displayed an emission peak at 522nm. This blue shift of emission wavelength was due to the affinity of dye molecules (NHS-FAM) with G-AgNPs, therefore making the electron transfer mechanism easier [23]. With clear indication from the graph, it shows that the as-prepared G-AgNPs excited at 468nm did not have any fluorescence.

A

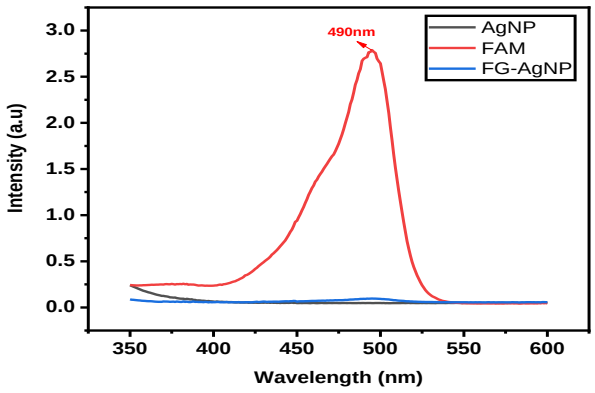

B

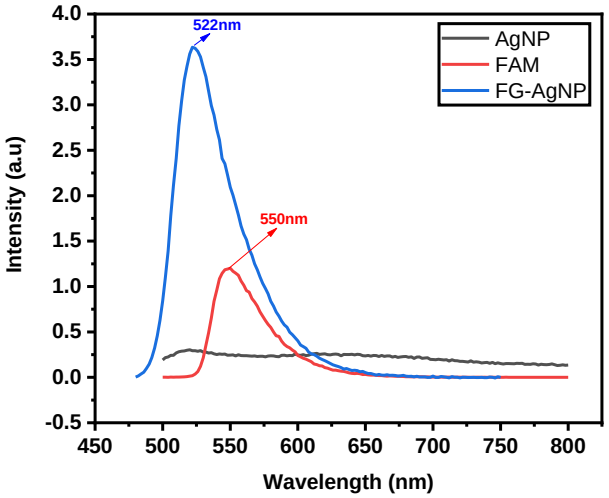

Fig. 3: A) Absorption spectra of G-AgNP, NHS-FAM and FG-AgNP, B) Emission spectra of AgNP, NHS-FAM, and FG-AgNP excited at 468nm.

Since NHS-FAM is pH-responsive, the fluorescence intensity at different pH was studied which is shown in fig. 4A. From the figure, it can be seen that the 550nm emission intensity increased significantly with an increase in pH from 5-7 under 468nm excitation. However, from pH 8-10, there was no significant increase in intensity as compared to pH 5-7 making NHS-FAM very responsive within a short range of pH. However, the fluorescence intensity of FG-AgNP at different pH increased with increment in pH values of 5-10 hence making it responsive over a wide pH range as shown in fig. 4B. Reversibility studies on FG-AgNP were performed by switching the pH between 6 and 10. As shown in fig. 4C, the fluorescence intensity at pH 6 decreased whiles switching the pH to 10 increased and this was repeated for about 4 cycles.

A

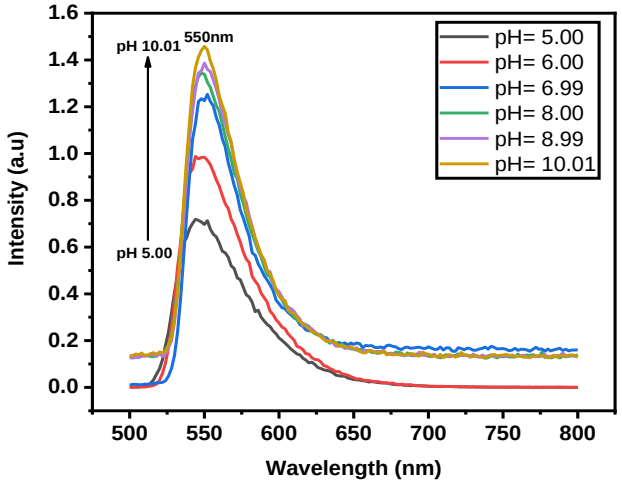

B

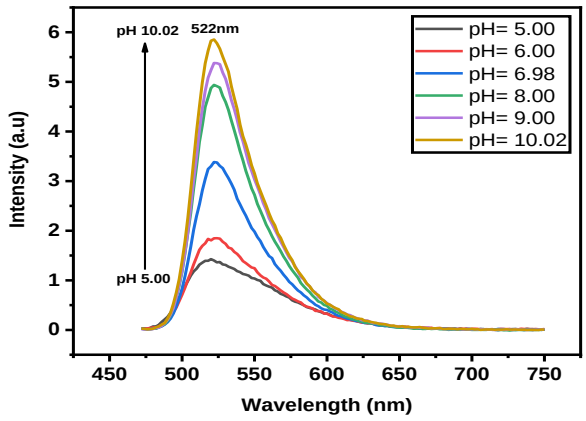

C

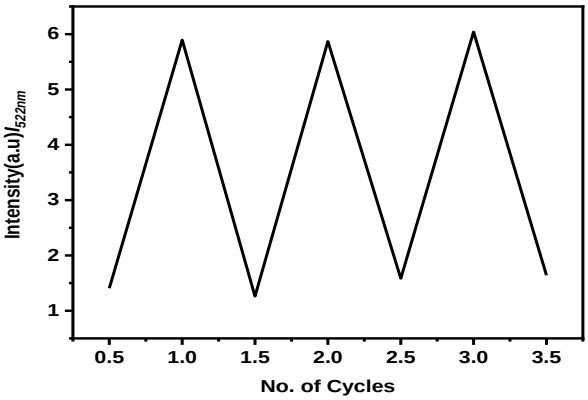

Fig. 4: Fluorescence spectra of A) NHS-FAM and B) FG-AgNP at different pH values. C) Reversibility studies on FG-AgNPs at pH between 6 and 10.

The fluorescence intensity of FG-AgNP became linearly dependent on pH as shown in fig. 5A. Comparing the linear dependency of FG-AgNP to NHS-FAM, it can be seen that FG-AgNP had a very good increase in intensity as pH increased from 5-10. This gave rise to a better linear regression (R^2) of 0.9992 for FG-AgNP as compared to 0.9608 for NHS-FAM. Hence, FG-AgNP is more responsive to a wide pH range than NHS-FAM.

A

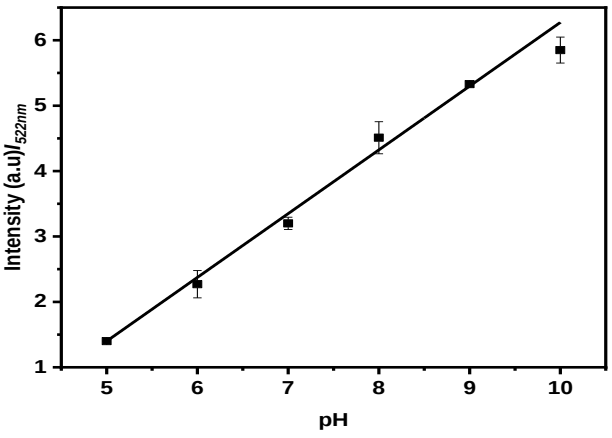

B

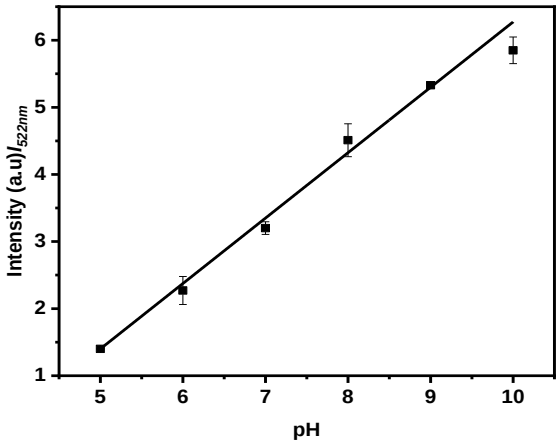

C

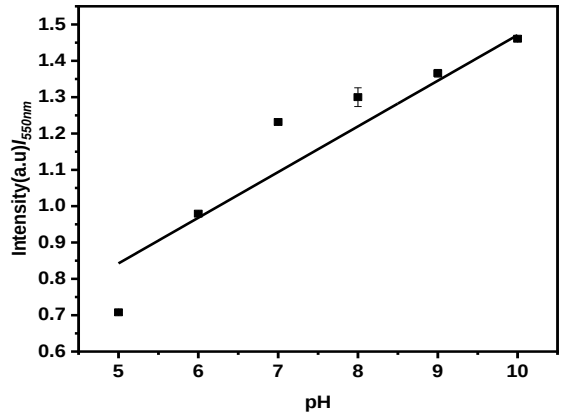

Fig. 5: Relationship between pH and fluorescence Intensity of A) FG-AgNP (I_{522nm}) and B) NHS-FAM (I_{550nm}).

After successful conjugation onto pH-sensitive dye (NHS-FAM) which increased the fluorescence intensity over a wide range of pH values, it was examined whether this observed reversible pH-dependent can be employed to pH insensitive dye (NHS-TAMRA). Conjugation onto G-AgNPs was straightforward and was first confirmed using agarose gel electrophoresis. As shown in fig. 6A, lane 1 which is a faint yellowish-brown colour indicates G-AgNPs, lane 2 which has a reddish-pink band shows the modified AgNPs (TG-AgNPs) and the free pinkish band in lane 3 indicates the pure monomeric NHS-TAMRA. The pure NHS-TAMRA and the G-AgNPs showed a difference in mobility with different band shapes as seen in the figure below whiles the G-AgNPs and TG-AgNPs had similar movement indicating conjugation was successful. Also confirming the conjugation, it can be seen that TG-AgNPs showed fluorescence under UV light which is shown in fig. 6B. Fig. 6C illustrates HR-TEM of TG-AgNPs with uniform size distribution and also having an average diameter of 2.22±0.58nm which is consistent with the core size of G-AgNPs (2.01±0.60nm) and also similar to that of FG-AgNPs.

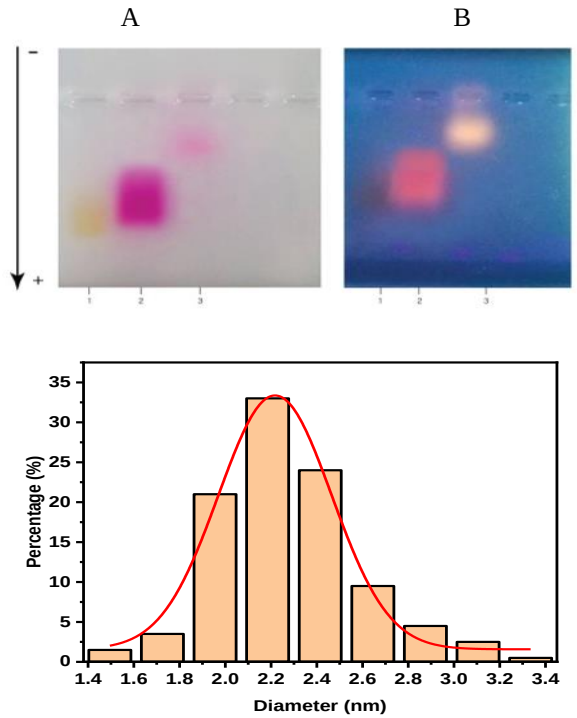

Fig. 6: Agarose gel electrophoresis of A) bright-field image B) under UV light image and C) HR-TEM image and Size distribution of TG-AgNP. Scale bar = 10nm.

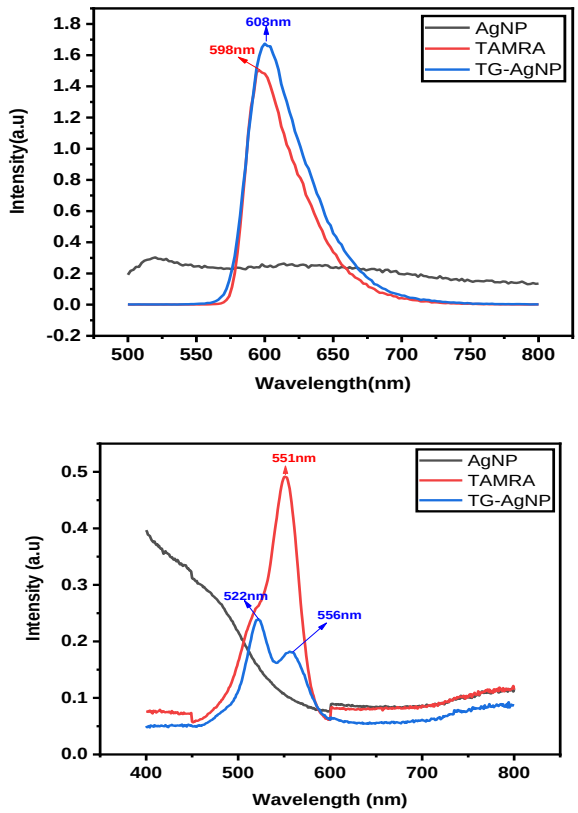

Fig. 7: A) Emission spectra of AgNP (Ex. 366nm), NHS-TAMRA (Ex. 406nm) and TG-AgNP (Ex. 398nm). B) Absorption spectra of AgNP, NHS-TAMRA, and TG-AgNP.

In fig. 7A, the fluorescence spectra of TG-AgNP showed an emission with maximum intensity observed at 608nm and comparing to the maximum emission (598nm) of the pure monomeric NHS-TAMRA, there is a blue 10nm shift in the emission of NHS-TAMRA after conjugated to G-AgNPs. This phenomenon demonstrates the dipole-dipole coupling among G-AgNP and the NHS TAMRA molecules [24], which was further confirmed using their UV/Vis absorption spectra.

As shown in fig. 7B, pure NHS-TAMRA displayed a strong absorption peak at 551nm and an additional small shoulder peak at 522nm which was due to the connection between pure monomeric NHS-TAMRA molecules in aqueous solution [25]. After conjugating NHS-TAMRA to G-AgNPs, the strong absorption peak at 551nm split into two peaks; one peak displayed at 522nm and the other was blue-shifted to 556nm. The higher peak at 522nm was due to the presence of G-AgNPs on NHS-TAMRA and also this observation further confirmed the dipole-dipole couplings of NHS-TAMRA molecules on G-AgNPs.

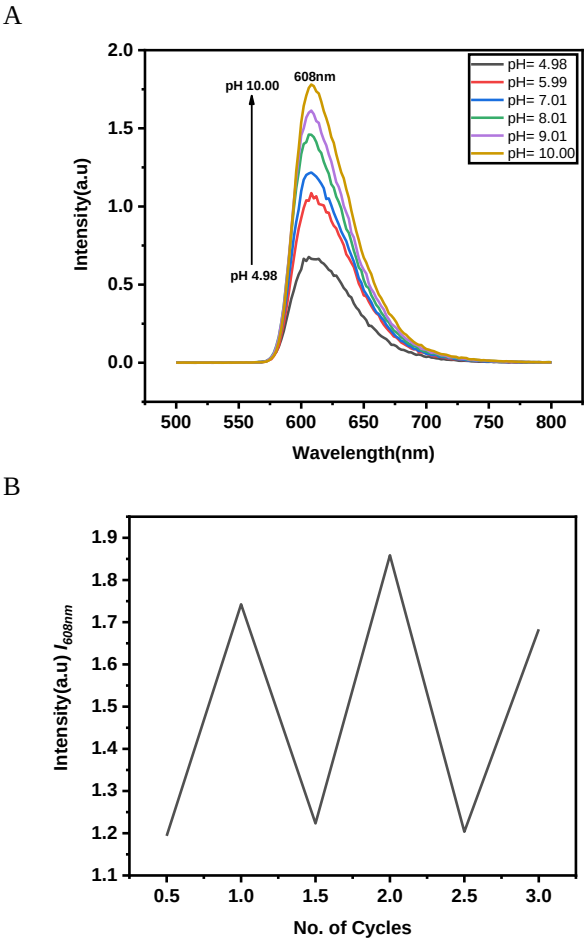

C

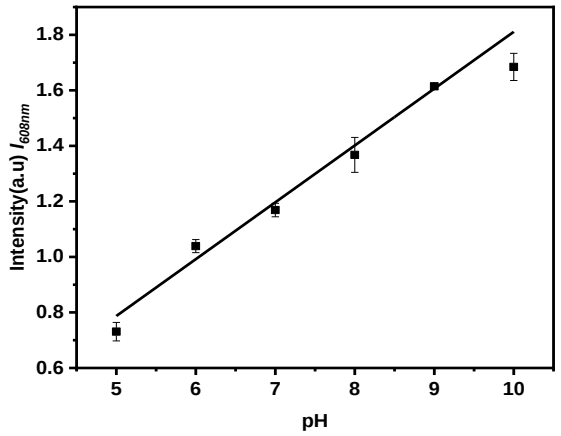

D

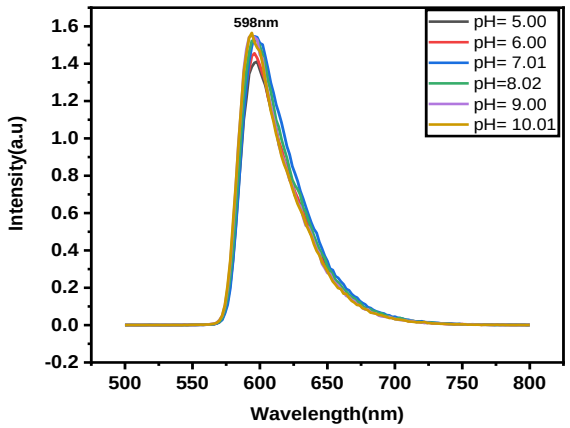

Fig. 8: A) Fluorescence spectra of NHS-TAMRA at different pH values. B) Fluorescence spectra of TG-AgNPs at different pH values. C) Reversibility studies on fluorescence intensity (I_{608nm}) of TG-AgNP with pH change between 6 and 10 and D) The relationship between pH and Intensity (I_{608nm}).

Since pure monomeric NHS-TAMRA is insensitive to pH, it wasn't expected to show a change in fluorescence intensity with different pH values as shown in fig. 3.8A. However, after conjugation of NHS-TAMRA to G-AgNPs, it exhibited a strong emission affinity to pH changes. As illustrated in fig. 8B, an increase in pH from 5-10 resulted in an increase of fluorescence intensity at 608nm. This significant increase in fluorescence intensity within the pH range of 5-10 makes TG-AgNP pH-responsive. Furthermore, this pH dependency is highly reversible as seen in fig. 8C where the pH is changed and measured simultaneously between 6 and 10. Fig. 8D shows how the fluorescence intensity of TG-AgNPs depends linearly on pH, with an increase in pH leading to increment in the fluorescence intensity. This gave a linear regression (R^2) value of 0.9866.

For the results obtained from the absorption and fluorescence spectra of TG-AgNPs, a scientific assumption was proposed as indicated in fig. 9. When hydroxide ions (-OH) are added to TG-AgNP which increases the pH value, the angle between the transition dipoles of the TAMRA dimer on G-AgNP increases slightly whiles the binding of the TAMRA dimer decreases due to the enhanced repulsion among the negatively charged GSH ligand. Hence, the emission intensity of TAMRA will increase rapidly with increasing pH and vice versa [25].

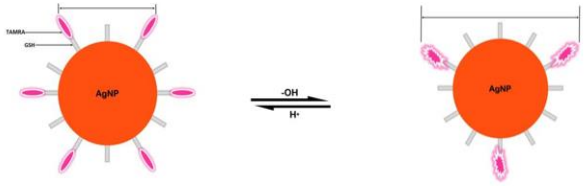

Fig. 9: A hypothesized pH-responsive mechanism of TG-AgNP.

IV. CONCLUSION

AgNPs capped with GSH were successfully conjugated onto NHS-FAM which was confirmed using agarose gel electrophoresis. Although NHS-FAM is a pH-sensitive dye, conjugation onto G-AgNPs (FG-AgNPs) produced a pH nanoprobe with an average size of 2.12±0.68nm which displayed fascinating sensitivity over a wide pH range. Since the as-prepared G-AgNPs was able to increase the range of a pH-responsive dye, it gave rise to the idea of experimenting with NHS-TAMRA.

In light of that, a pH nanoprobe with an average size of 2.22±0.58nm and possessing fluorescent properties where NHS-TAMRA was conjugated onto small-sized G-AgNPs (2nm) were constructed. This resulted in a characteristic improvement that makes TG-AgNP show linear dependency on pH values 5-10.

Finally, future works can be done using the as-prepared nanoprobe for intracellular findings for pH sensing and also, temperature sensing characteristics of silver nanoparticles conjugated with the used organic dyes can be examined.

ACKNOWLEDGMENT

Firstly, I would like to thank the almighty God for giving me strength and also thank my academic supervisor Dr. Sun Shasha for her encouraging guidance and constructive support throughout my stay in Jiangsu University of Science and Technology.

Secondly, I appreciate the support given to me by my laboratory mates and also thank the School of Overseas department for providing financial support throughout my stay in Jiangsu University of Science and Technology.

Finally, I would like to thank my mother, Felicia Owusu, my friends; Kodwo Pobee, Benjamin Panful, Prosper Amuzu, Bismark Okanta, Jehu Apaflo and my dear Taonga Evelyn Mpingilwa for their great love and support to reach this height.

REFERENCES

[1] B. O. Noqtah, "pH effect on the aggregation of silver nanoparticles synthesized by chemical reduction," Versita, vol. 32, no. 1, pp. 107–111, 2014.

[2] O. V Salata, "Applications of nanoparticles in biology and medicine," J. Nanobiotechnology, vol. 6, pp. 1–6, 2004.

[3] V. V Mody, R. Siwale, A. Singh, and H. R. Mody, "Introduction to metallic nanoparticles," Pharm. bioallied Sci., vol. 2, no. 4, 2010.

[4] J. Dobson, "Gene therapy progress and prospects: Magnetic nanoparticle-based gene delivery," Gene Ther., vol. 13, no. 4, pp. 283–287, 2006.

[5] S. Rudge, C. Peterson, C. Vesely, J. Koda, S. Stevens, and L. Catterall, "Adsorption and desorption of chemotherapeutic drugs from a magnetically targeted carrier (MTC)," J. Control. Release, vol. 74, no. 1–3, pp. 335–340, 2001.

[6] J. Natsuki, T. Natsuki, and Y. Hashimoto, "A Review of Silver Nanoparticles : Synthesis Methods, Properties, and Applications," Int. J. Mater. Sci. Appl., vol. 4, no. 5, pp. 325–332, 2015.

[7] A. Syafiuddin, Salmiati, M. R. Salim, A. H. Kueh, T. Hadibarata, and H. Nur, "A Review of Silver Nanoparticles: Research Trends, Global Consumption, Synthesis, Properties, and Future Challenges," J. Chin. Chem. Soc, vol. 64, pp. 732–756, 2017.

[8] Q. H. Tran, V. Q. Nguyen, and A. Le, "Silver nanoparticles : synthesis, properties, toxicology, applications and perspectives," Adv. Nat. Sci., vol. 4, p. 20, 2013.

[9] K. Lee and M. A. El-Sayed, "Gold and Silver Nanoparticles in Sensing and Imaging : Sensitivity of Plasmon Response to Size, Shape, and Metal Composition," J. Phys. Chem, vol. 110, pp. 19220–19225, 2006.

[10] L. R. Hirsch et al., "Nanoshell-mediated near-infrared thermal therapy of tumors under magnetic resonance guidance," P. Natl. Acad. Sci., vol. 100, no. 23, pp. 13549–13554, 2003.

[11] D. A. Stuart, A. J. Haes, C. R. Yonzon, E. M. Hicks, and R. P. Van Duyne, "Biological applications of localized surface plasmonic phenomena," Nanobiotecnol., vol. 152, no. 1, pp. 13–32, 2005.

[12] X. Zhang, Z. Liu, W. Shen, and S. Gurunathan, "Silver Nanoparticles : Synthesis, Characterization, Properties, Applications, and Therapeutic Approaches," Int. J. Mol. Sci., vol. 17, p. 1534, 2016.

[13] C. Caro, P. M., R. Klippstein, D. Pozo, and A. P., "Silver Nanoparticles: Sensing and Imaging Applications," Silver Nanoparticles, pp. 201–224, 2010.

[14] H. D. Beyene, A. A. Werkneh, H. K. Bezabh, and T. G. Ambaye, "Synthesis paradigm and applications of silver nanoparticles (AgNPs)," Sustain. Mater. Technol., 2017.

[15] J. Han and K. Burgess, "Fluorescent Indicators for Intracellular pH - Chemical Reviews," Chem. Rev., vol. 110, no. 5, pp. 2709–2728, 2010.

[16] H. R. Kermis, Y. Kostov, G. Rao, and B. Engineering, "Analyst Sensor," RSC Anal., vol. 128, pp. 1181–1186, 2003.

[17] A. Iovescu et al., "Ageing of fluorescent and smart naphthalene labeled poly(acrylic acid)/cationic surfactant complex," Colloids Surfaces A Physicochem. Eng. Asp., 2017.

[18] P. K. Ang, W. Chen, A. Thye, S. Wee, and K. P. Loh, "Solution-Gated Epitaxial Graphene as pH Sensor," Am. Chem. Soc., vol. 130, pp. 14392–14393, 2008.

[19] Z. Yang et al., "Fluorescent pH sensor constructed from a heteroatom-containing luminogen with tunable AIE and ICT characteristics," RSC Chem. Sci., 2013.

[20] Y. Lu and B. Yan, "A ratiometric fluorescent pH sensor based on nanoscale metal-organic frameworks (MOFs) modified by europium(III) complexes," ChemComm., vol. 253, pp. 13323–13326, 2014.

[21] L. Ferrari, L. Rovati, P. Fabbri, and F. Pilati, "Disposable Fluorescence Optical pH Sensor for Near Neutral Solutions," Sensors, vol. 13, pp. 484–499, 2013.

[22] H. Ramsay, D. Simon, E. Steele, A. Hebert, R. D. Oleschuk, and K. G. Stamplecoskie, "The power of fluorescence excitation-emission matrix (EEM) spectroscopy in the identification and characterization of complex mixtures of fluorescent silver clusters," RSC Adv., vol. 8, no. 73, pp. 42080–42086, 2018.

[23] S. Kalele, A. C. Deshpande, S. B. Singh, and S. K. Kulkarni, "Tuning luminescence intensity of RHO6G dye using silver nanoparticles," Bull. Mater. Sci., vol. 31, no. 3, pp. 541–544, 2008.

[24] J. Zhang and J. R. Lakowicz, "Enhanced Luminescence of Phenyl-phenanthridine Dye on Aggregated Small Silver Nanoparticles," J. Phys. Chem, vol. 109, pp. 8701–8706, 2005.

[25] S. Sun, X. Ning, G. Zhang, Y. Wang, C. Peng, and J. Zheng, "Dimerization of Organic Dyes on Luminescent Gold Nanoparticles for Ratiometric pH Sensing Zuschriften Angewandte," Angew. Chemie - Int. Ed., vol. 128, pp. 2467–2470, 2016.

Author Profile

Mr. Joseph Afrifa Owusu obtained a Bachelor of Science degree in Chemistry from the Kwame Nkrumah University of Science and Technology in 2014. He was an active member of the Ghana Students Chemical Society where he won many awards in research and experimental work. He further moved on to work as a Quality Control Chemist at Kinapharma Pharmaceutical Company Limited in Ghana. From there he pursued my education in Master of Science degree program in Chemical Engineering and Technology from the Jiangsu University of Science and Technology.

